MATERIALE PLASTICE
https://revmaterialeplastice.ro
https://doi.org/10.37358/Mat.Plast.1964

Morphology and Mechanical Properties of Polyethylene Terephthalate/Ethylene Propylene Diene Monomer (PET/EPDM) in the Presence of Nanoclay

BAIFEN LIU[1], MOHAMMAD MIRJALILI[2*], PEIMAN VALIPOUR[3], SAJAD PORZAL[2], SHIRIN NOURBAKHSH[4]

[1]School of Information Engineering, Gongqing Institute of Science and Technology, Jiujiang, Jiangxi, China
[2]Department of Textile and Polymer Engineering, Yazd Branch, Islamic Azad University, Yazd, Iran
[3]Department of Textile, Apparel Engineering, Qaemshaher Branch, Islamic Azad University, Qaemshahr, Iran
[4]Textile Department, Yadegare Imam Khomeini (RAH) Shahr-e-Rey Branch, Islamic Azad University, Tehran, Iran

Abstract: *This research deals with the mechanical properties, microstructure, and interrelations of triple nanocomposite based on PET/EPDM/Nanoclay. These properties were examined in different percentages of PET/EPDM blend with compatibilizer (Styrene-Ethylene/Butylene-Styrene)-G-(Maleic anhydrate) (SEBS-g-MAH). Results showed that the addition of 15% SEBS-g-MAH improved the toughness and impact strength of this nanocomposite. SEM micrographs indicated the most stable fuzzy microstructure in a 50/50 mixture of scattered phases of EPDM/SEBS-g-MAH. The effects of percentages of 1, 3, 5, 7 nanoclay Cloisite 30B (C30B) on the improvement of the properties were evaluated. With the addition of nano clay, the toughness and impact strength was reduced. Thermal destruction of nanoclay in processing temperature led to the decreasing dispersion of clay plates in the matrix and a reduction in the distances of nano clay plates in the composite compared to pure nano clay. XRD and TEM analysis was used to demonstrate the results. By adding 1% of nanoclay to the optimal sample, maximum stiffness, and Impact strength, among other nanocomposites, was achieved.*

Keywords: *Microstructure, Mechanical properties, nanocomposite, PET/EPDM/Nanoclay*

1. Introduction

Polyethylene terephthalate (PET) is a synthetic polymer with unique mechanical and chemical properties such as high strength and modulus, and high processability characteristics such as low permeability to solvents and gases, electrical properties, and resistance to tearing and chemicals [1-7]. However, this substance has certain disadvantages, such as sensitivity to cracks [8] and low strength against atmospheric factors. Therefore, engineers are trying to increase the toughness of this polymer with the addition of an elastomeric phase to overcome the mentioned shortages [9-18]. One way to improve the mentioned properties is to add an elastomeric phase to increase the toughness [19, 20]. Therefore, the use of EPDM with properties such as improving toughness, ozone resistance [21], and impact strength can be the right solution. Since PET/EPDM alloy is thermodynamically incommensurable and forms a multi-phase morphology after alloying [22, 23], a compatibilizer is required to obtain optimal properties and to control morphology and cohesion between the phases [24].

In order to improve the compatibility of PET to EPDM, Styrene-Ethylene/Butylene-Styrene-G-Maleic anhydrate (SEBS-g-MAH) was used. The elastomeric phase affects various properties, including modulus and stiffness. Therefore, some of the shortcomings can be compensated with the addition of reinforcing agents. Indeed, properties such as modulus, impact strength, and stiffness are simultaneously improved with the formation of Nanocomposite structure [25]. According to previous researches, using traditional reinforcing agents such as soot, which increases elastomeric properties in high weight percentages, leads to certain shortcomings in final products and increased weight [26]. However, using nano clay particles, which have reinforcing properties even in low weight percentages, results in decreased weight and the final cost of the product [27-29]. According to another study, the stretch strength of nanoclay-EPDM composites is three to four times as much as pure plastic [30].

**email: Dr.mirjalili@iauyazd.ac.ir, m.mirjalili@mail.ru*

However, increasing nanoclay content over 5% leads to the squishing of nanoparticles and decreases stretch strength. This property was observed in other studies [31]. Entezam et al. investigated the effect of the presence of nanoclay in PP/ PET alloy. They observed that the dispersion of nano clay particles into the matrix phase affects crystallization temperature and stretch modulus and strength and improved mechanical properties [32]. Jadi et al. investigated the effect of Cloisite 30B (C30B) and Cloisite 15A in EPDM/SAN nanocomposite and observed that up to 5% of C30B could reduce the diameter of EPDM particles and results in better dispersion of the particles in SAN phase [33]. Some other works showed a relationship between viscoelastic behavior and morphology of SR/ EPDM/ Nanoclay nanocomposite in the presence of Maleic Anhydrate. Nano clay showed better dispersion in the EPDM phase, compared to SR, and had a better structure in comparison with the sample without compatibilizer [34]. The present study examined the significant factors on the formation and control of morphology and their relationship with the mechanical properties of triple nanocomposites based on PET/EPDM/Nanoclay using SEBS-g-MAH as compatibilizer.

2. Materials and methods

In the present study, PET was purchased from Hualon Co., Korea. EPDM was prepared from Exxonmobil, Belgium. Ethylene,SEBS-g-MAH was from Kraton Polymer Group, USA. C30B was used from Southern Clay Products, USA.

2.1. Sample preparation

All samples PET, EPDM, SEBS-g-MAH, and C30B were weighted using a digital scale according to the following formulation: PET granule and C30B were dried in a vacuum oven at 120°C for 8 and 6 h, respectively. Then, PET was removed from the oven and was mixed with EPDM at an internal mixer at 260°C, 600 rpm for 9 min, according to the formulation in Table 1. The same trend was repeated in 3 steps for PET/ EDPM/ SEBS-g-MAH and four steps for PET/ EDPM/ SEBS-g-MAH/ C30B. All the six mixtures were cooled at room temperature, and then sample sheets were prepared at 260 °C for 5 min after 2 min preheating by using a compressive molding machine (type p200p) made by Dr.Collin Co., Germany, for further tests.

Table1. Samples Formulation.

Sample Code	PET	EPDM	SEBS-MA	Cloisite 30B (C30B)
a	100	0	0	0
b	70	30	0	0
c	70	22.5	7.5	0
d	70	15	15	0
e	70	7.5	22.5	0
f	69.3	14.85	14.85	1
g	67.9	14.55	14.55	3
h	66.5	14.25	14.25	5
j	65.1	13.95	13.95	7

2.2. Impact Test

The impact strength was examined using the Charpy method. The standard method of ISO 179 under the angle of 124.4 °C was used.

2.3. Tensile Test

Standard ASTM D412 measured tensile, and strain strength of the blend samples at room temperature with a stretch rate of 50 mm/min, and the average results were reported.

2.4. Transmission Electron Microscopy (TEM)

A skinny layer with an approximate thickness of 100 nm was put at liquid nitrogen under refrigeration conditions and was cut using EM UC/FC6ULTRAMICROTOME Tool (lecia) equipped

with a diamond knife. Then TEM images were obtained using a Transmission electron microscope KEV 80 of EM 900 model made by Ziess Co. at accelerating voltage of 80 KV [35-41].

2.5. X-Ray Diffraction (XRD)

In XRD analysis, the layered silicate structure of C30B, the distance between nanoclay plates, and the morphology of the obtained nanocomposites were examined using X'Pert Pro MPD machine, accelerator voltage of 50 KV, and a current of 40 mA. The diffraction spectrum was obtained at 20 between 2-10 °C, and the distance between the layers is obtained according to Bragg's Law (1):

$$d= \gamma/2\sin\theta max \quad (1)$$

where γ is the wavelength.

2.6. Scanning Electron Microscopy (SEM)

This technique was used for direct observation and assessment of the layered microstructure of the blend samples. Samples were broken in liquid nitrogen and were coated with a gold film.

3. Results and discussions

3.1. Mechanical Properties of the Nanocomposite Polymer

3.1.1. Impact and tensile tests

The results of the Impact and tensile tests were presented in Table 2.

Table 2. Mechanical properties (Impact, tensile strength, and elongation to tear point) of PET/ EDPM/ SEBS-g-MAH/ C30B with different content percentages

Sample Code	Sample	Impact Strength (kj/m^2)	TensileStrength (MPA)	Elongation (%)
a	PET	0.7	16.25	6
b	PET/EPDM (70/30)	1.4	10.54	5.55
c	PET/EPDM/SEBS-MA (70/22.5/7.5)	2.1	6.11	4.62
d	PET/EPDM/SEBS-MA (70/15/15)	3	8.23	4.40
e	PET/EPDM/SEBS-MA (70/7.5/22.5)	2.2	18.29	7.55
f	PET/EPDM/SEBS-MA/ C30B (69.3/14.85/14.85/1)	2.83	12.97	8.16
g	PET/EPDM/SEBS-MA/ C30B (67.9/14.55/14.55/3)	2.5	5.31	3.40
h	PET/EPDM/SEBS-MA/ C30B (66.5/14.25/14.25/5)	2.7	3.59	4.39
j	PET/EPDM/SEBS-MA/ C30B (65.1/13.95/13.95/7)	1.65	4.55	4.05

There can be seen that the toughness and impact strength has improved with the addition of 30% of elastomeric phase (EPDM) to the matrix (PET), which is fragile [42] (mixture *b)*, while tensile strength was decreased, which is due to incompatibility of the two components and low cohesion between the surfaces. Moreover, elongation was also increased, an indication of higher toughness and structural conflict. Since PET and EPDM are incommensurable, SEBS-g-MAH was used as a compatibilizer. It decreased the EPDM phase of 22.5%, and with the addition of 7.5% of SEBS-g-MAH(Mixture *c)*, it can be observed that toughness and impact strength was improved due to the increased dispersion of the EPDM phase in PET and smaller particles (EPDM), which is observable in SEM images. However,

tensile strength and elongation were decreased. It is also implied that impact strength and elongation are negatively correlated, indicating the increase in toughness.

It is observed that maximum toughness and impact strength can be achieved with a further reduction of the EPDM phase to 15% and the addition of 15% of SEBS-g-MAH (mixture *d*). This shows that the most stable fuzzy microstructure is achieved at a 50/50 mixture of dispersed phases (EPDM/SEBS-g-MAH), as shown in SEM images. Furthermore, tensile strength has also increased while elongation was decreased, indicating increased toughness and impact strength. Next, with the addition of the EPDM phase and SEBS-g-MAH to 7.5 and 22.5% (mixture *e*), it can be observed that toughness and impact strength is reduced because the increased SEBS-g-MAH in the mixture leads to reduced dispersion and smaller size of particles of EPDM phase in PET. This can be seen in SEM images. Also, tensile strength and elongation have increased, indicating reduced toughness and impact strength.

Next, the mixture *d* is selected due to maximal toughness and Impact strength and the most stable fuzzy microstructure, in which EPDM and SEBS-g-MAH have equal content percentages. With the addition of C30B with different percentages, the effect of nanocaly particles on the mechanical and fuzzy microstructure of the blend was examined. With the addition of 1% of C30B to optimal sample (mixture *f),* toughness and Impact strength were reduced because the effect of compatibilizer on the dispersion of nanoparticles in PET is minimal and leads to layered dispersion of clay in the polymer matrix. Moreover, the intermediate tensile between the PET phase and the dispersed phase (EPDM) was decreased, but a considerable amount of nanoparticles were seen in the phase's interface, which is observed in SEM images. Moreover, tensile strength was increased because the addition of organic agent-modified clay led to a reduction of the size of micronic regions of the dispersed phase. However, elongation was also observed, which is due to decreased toughness and impact strength.

With increasing nanoclay content to 3%(mixture *g),* it can be observed that toughness and impact strength were decreased due to the small effect of compatibilizer on the dispersion of clay layers and also weak interaction of these layers with the matrix and dispersed phases. However, tensile strength and elongation were increased because the addition of organic agent-modified clay led to an increase in the size of Micronics regions of the dispersed phase and the presence of silicate masses. With the further addition of nanoclay content to 5% (mixture *h),* it can be observed that toughness and impact strength were increased because a more considerable amount of clay was layered, the concentration of nanoparticles in the polymer matrix decreased, and layered dispersion of nanoplates in polymer matrix increased.

Furthermore, tensile strength was decreased due to the reduced presence of silicate masses, while elongation was also increased. Then, with further addition of nanoclay content 7% (mixture *j),* it can be observed that toughness and impact strength were decreased because only a small amount of clay was layered and the concentration of nanoparticles in the polymer matrix reached the maximum. Moreover, tensile strength was increased, but elongation decreased.

3.2. Morphology and Microstructure of Nanocomposite Polymer

3.2.1. Examining the microstructure and morphology using SEM

Figure 1(b) shows the morphology of PET/ EPDM mixture. The matrix-disperse morphology reveals that when the dispersed phase (EPDM) has a lower viscosity than the PET phase, it is dispersed uniformly in the form of small droplets. Here, the size of the dispersed phase (EPDM) is fairly large due to inappropriate commensurability, leading to non-uniform dispersion. Moreover, due to the incompatibility of the two components, cohesion is fragile in the interface, and the two phases are separated.

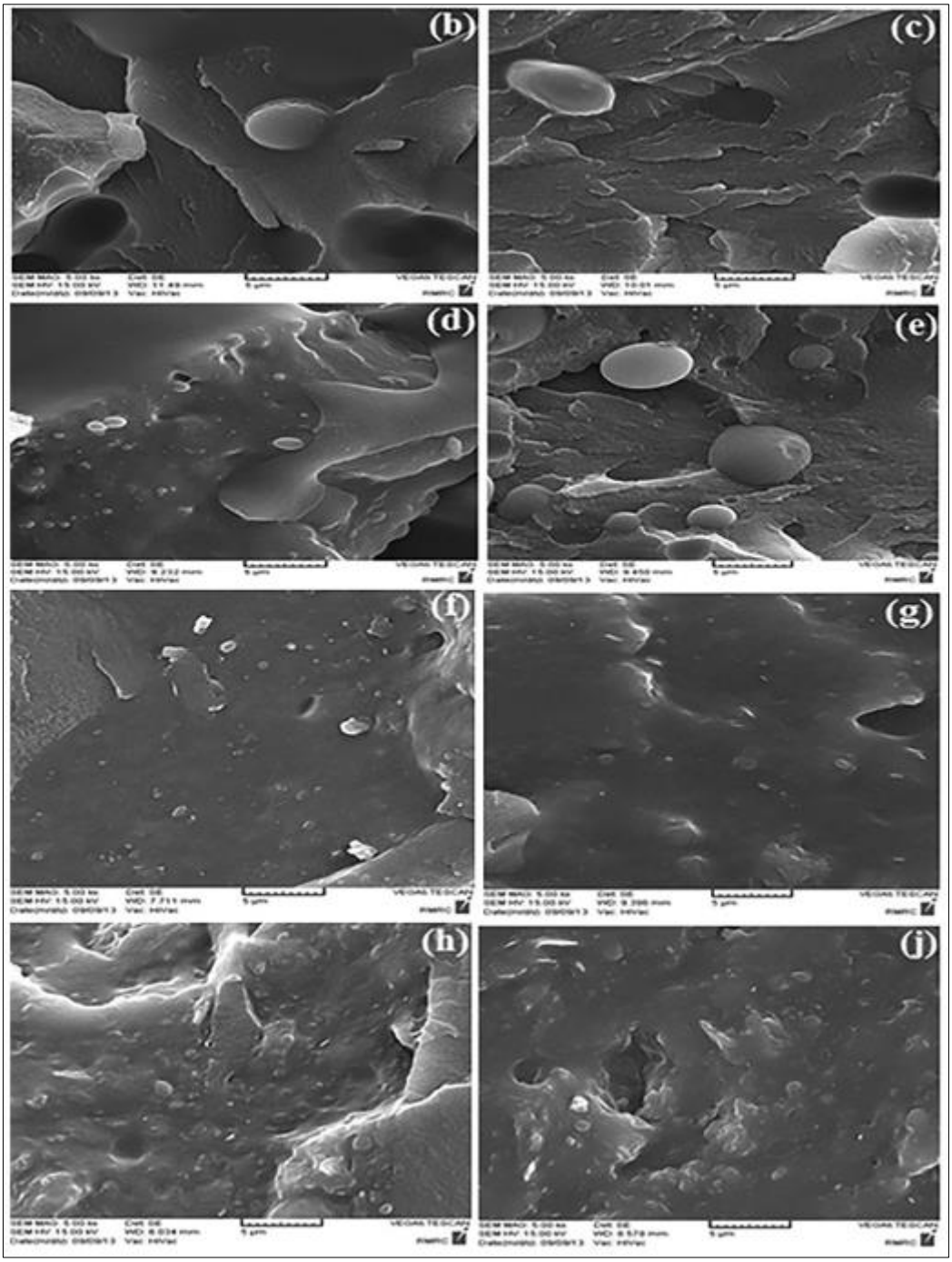

Figure 1. SEM image of failure surface in b) PET/ EPDM (70/30), c) PET/ EPDM/SEBS-MA (70/22.5/ 7.5), d) PET/EPDM/SEBS-MA (70/15/15), e) PET/EPDM/SEBS-MA (70/7.5/22.5), f) PET/EPDM/SEBS-MA/ C30B (69.3/14.85/14.85/1), g) PET/EPDM/SEBS-MA/ C30B (67.9/14.55/14.55/3), h) PET/EPDM/SEBS-MA/ C30B (66.5/14.25/14.25/5), j) PET/ EPDM/SEBS-MA/ C30B (65.1/13.95/13.95/7)

In all content percentages of compatibilizer, Figure 1(c-e), dispersed phase (EPDM), and SEBS-g-MAH are observed as separated phases in the matrix. As shown in the image, elastomeric particles are torn under stress, and cavities have been formed. Since the matrix and the interface of the two phases are strong, SEBS-g-MAH particles are oriented to these cavities, indicating that shear stress has been maximal; hence tensile strength has considerably increased. However, with the reduction in impact strength, elongation has also increased. Therefore, with the further addition of SEBS-g-MAH to 15%, it

can be observed that the maximum dispersion of EDPM is achieved, and the particles of the dispersed phase are considerably smaller and are in the form of an oval.

Figure 1(f-j) shows the effect of the addition of various percentages of C30B (1, 3, 5, and 7) to the mixture PET/ EPDM/ SEBS-g-MAH. Moreover, nanoparticles resulted in a better dispersion of EPDM in PET (layered dispersion) with the most inter surface effects between the matrix and silicate layers compared to other nanocomposites. Therefore as it is evident in TEM images, the mixture has the most impact strength. Furthermore, the percentage of the dispersed phase (EPDM) and SEBS-g-MAH is equal, and it is observed that by adding 1% of clay, the compatibilizing effect of nanoparticles on decreasing the size of dispersed phase particles is crystal clear. Indeed, particles have become smaller, and their tensile has also decreased.

Moreover, the addition of organically-modified clay reduced the size of micronic regions of the dispersed phase (EPDM), which indicated a reduction of shear stress. As a result, impact strength has decreased compared to the optimal sample. Also, the images (g-j) show that in this percentage of clay, the role of compatibilizer in layering clay sheets and dispersion of nanoparticles in the matrix and the interface is minimal, leading to reduced cohesion between the two phases. This can be due to increased interactions between the active agents in the modified clay and maleic anhydride (SEBS-g-MAH).

3.3. Investigation of microstructure using X-Ray Diffraction (XRD)

Table 3. Properties of nanoparticles.

d001 (nm)	20 (˚C)	Concentration of reformer (meq/100g clay)	Structure of reformer	Organic reformer	Cloisite
18/5	4/8	90	Ch3-N+ (CH2CH2OH)2-T	MT2EtOH	30b

Table 4. Features and content percentage of the samples containing Cloisite 30B (C30B).

Sample Code	**20 (˚C)**	**d001 (nm)**
f	6.099	1.4478
g	5.98	1.4767
h	5.849	1.5098
j	5.859	1.5072

Results of XRD test for examining the microstructure of pure C30B are presented in Tables 3 and 4. As shown in Tables 3 and 4, in samples containing C30B, the feature peak is displaced to larger angles rather than pure clay. This indicates the decrease in the distance between nanoclay sheets in the composite compared with the pure clay. This seems to be due to the thermal destruction of active organic agents connected to C30B at a processing temperature of 260°C [43]. It reduced layered dispersion of clay sheets in the polymer matrix and decreased the distance between nanoclay sheets in the nanocomposite compared to pure nanoclay [44].

Based on the results from Figure 2, it can be stated that with the addition of 1% of C30B to the composite PET/EPDM/SEBS-g-MAH (70/15/15), the distance between the layers of nanoclay particles in the blend PET/EPDM decreases from 1.85 nm (pure C30B) to 1.447 nm (in mixture *f*). Therefore, XRD results reveal that PET and EPDM chains are not permeable to layers of C30B particles and do not have the compatibility of creating an interlayer structure for these particles; furthermore, the smaller layer distance for C30B particles can be attributed to the lower compatibility of PET and EPDM chains to C30B particles.

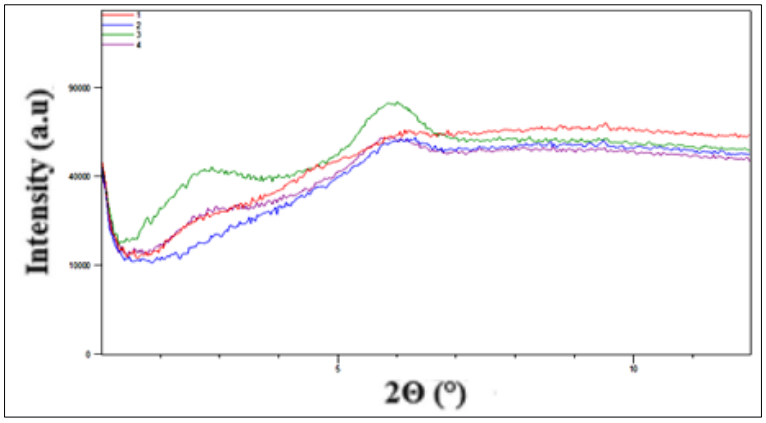

Figure 2. Diagrams obtained from XRD test for nanocomposites containing: f) PET/EPDM/SEBS-MA/ C30B (69.3/14.85/14.85/1); g) PET/EPDM/SEBS-MA/Closite 30b (67.9/14.55/ 14.55/3); h) PET/EPDM/SEBS-MA/ C30B (66.5/14.25/14.25/5); j) PET/EPDM/SEBS-MA/C30B

This also indicates an improper dispersion of nanoparticles in the matrix phase in this sample. This can be because of a large amount of the clay in this sample, which is layered, and almost all nanoclay particles are transmitted to the interface between the two phases, leading to the formation of a pseudo-network structure.

With increasing clay content to 3 and 5%, it can be seen that the feature peak of nanoclay particles goes to the smaller angle in nanocomposites. This shows an increased layer distance from 1.447 to 1.476 nm and 1.476, respectively. This indicates interlayer dispersion of nanoparticles of C30B in nanocomposites, which is due to the penetrability of PET and EPDM chains to layers of C30B. In this mixture, some of the nanoparticles move from the interface of the two phases (PET/EPDM) to the matrix phase. With the further addition of clay content to 7%, it is observed that the feature peak moves towards the greater angle in the nanocomposite, indicating a reduced distance between the layers of nanoclay particles to 1.507 nm. However, most nanoparticles moved from the interface of the two phases in the matrix. This indicates less interlayer dispersion for C30B nanoparticles in nanocomposite *j*, which is caused by less penetrability of PET and EPDM chains to the layers of C30B particles [45-53].

3.3.1. Investigating the microstructure and morphology using a transmission electron microscope (TEM)

Figure 3 presents TEM images with different magnifications for a nanocomposite sample PET/EPDM/SEBS-g-ma/ C30B containing 1% of nanoclay content. Almost all the nanoclay particles were observed in the interface of the two phases.

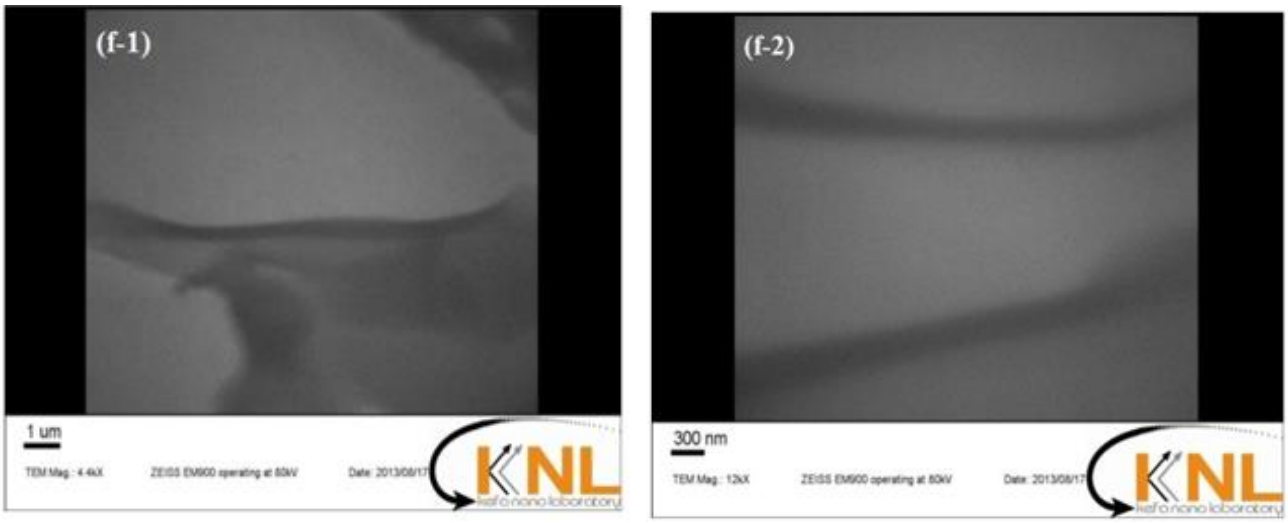

Figure 3. TEM images with manifications of 1 nm and 300 nm for nanocomposite e) PET/EPDM/ SEBS-g-MAH/C30B (69.3/ 14.85/ 14.85/ 1)

Based on the observations in Figure 3, nanoclay particles in this nanocomposite sample, containing 1% of nanoparticles, have a uniform distribution in the interface of the two phases in a way that nanoparticles covered almost all the surface of the interface. This indicates that there is not a proper dispersion of C30B nanoparticles in the PET phase [54-55].

4. Conclusions

The mechanical properties, microstructure of triple polymer nanocomposite based on PET/EPDM/ C30B were studied. In the PET/EPDM blend, toughness, and impact strength have increased, but since the two phases are incommensurable, the tensile strength decreased, leading to increased elongation. In order to compatibilizing the thermoplastic PET phase with the EPDM phase, SEBS-g-MAH was used as a compatibilizer. It was observed that with the addition of 15% of SEBS-g-MAH to the PET/EPDM blend, toughness and Impact strength reached their peaks in this nanocomposite. This means that the most stable fuzzy microstructure was achieved in a 50/50 mixture of dispersed phases (EPDM/SEBS-g-MAH), which is observable in SEM images. Also, with the addition of nano clay, the toughness and impact strength was reduced because the effect of compatibilizer in the dispersion of nanoparticles in the matrix is shallow; also, thermal destruction of nanoclay in processing temperature leads to the decrease dispersion of clay plates in the matrix and a reduction in the distances of nano clay plates in the composite compared to pure nano clay. These results are shown in XRD and TEM images. Addition of 1% of nanoclay to optimal sample, maximum stiffness, and impact strength among other nano-composites achieved.

References

1.AGLIETTO, M., COLTELLI, M. B., SAVI, S., LOCHIATTO, F., CIARDELLI, F., GIANI, M., Postconsumer polyethylene terephthalate (PET)/polyolefin blends through reactive processing. J. Mater. Cycles. Waste. Manage., 6(1), 2004, 13–19.
2.EVSTATIEV, M., FAKIROV, S., KRASTEVA, B., FRIEDRICH, K., COVAS, J. A., CUNHA, A. M., Recycling of poly (ethylene terephthalate) as polymer-polymer composites. Polym. Eng. Sic., 42(4)2002, 826–835.
3.ZUO, C., CHEN, Q., TIAN, L., WALLER, L., ASUNDI, A., Transport of intensity phase retrieval and computational imaging for partially coherent fields: The phase space perspective. Opt. Lasers Eng., 71, 2015, 20-32.
4.ZUO, C., SUN, J., LI, J., ZHANG, J., ASUNDI, A., CHEN, Q., High-resolution transport-of-intensity quantitative phase microscopy with annular illumination. Sci. Rep., 7(1), 2017, 7622-7654.
5.CAI, C., WU, X., LIU, W., ZHU, W., CHEN, H., QIU, J. C. D., SUN, C. N., LIU, J., WEI, Q., SHI, Y., Selective laser melting of near-α titanium alloy Ti-6Al-2Zr-1Mo-1V: Parameter optimization, heat treatment and mechanical performance. J. Mater. Sci. Technol., 57, 2020, 51-64.
6. CAI, C., TEY, W. S., CHEN, J., ZHU, W., LIU, X., LIU, T., ZHAO, L., ZHOU, K., Comparative study on 3D printing of polyamide 12 by selective laser sintering and multi jet fusion. J. Mater. Process. Technol., 288, 2020, 116882.
7. YANG, L., CHEN, M., WANG, J., QIAO, Y., GUO, P., ZHU, S., WANG, F., Microstructure and composition evolution of a single-crystal superalloy caused by elements interdiffusion with an overlay NiCrAlY coating on oxidation. J. Mater. Sci. Technol., 45, 2020, 49-58.
8.KHATIBI, M. A., AREFAZAR, A., ESFANDEH, M., Microstructure and properties of PET/EPDM, EPDM-gMA/organoclay ternary hybrid Nano composites: effect of blending sequence. Polymer., 8(1), 2008, 1874-1882.
9.CHEN, S., HASSANZADEH-AGHDAM, M. K., ANSARI, R., An analytical model for elastic modulus calculation of SiC whisker-reinforced hybrid metal matrix nanocomposite containing SiC nanoparticles. J. Alloys Compd., 767, 2018, 632-641.

10.ZHU, W., ZHANG, Z., CHEN, D., CHAI, W., CHEN, D., ZHANG, J., ZHANG, C., HAO, Y., Interfacial Voids Trigger Carbon-Based, All-Inorganic CsPbIBr2 Perovskite Solar Cells with Photovoltage Exceeding 1.33 V. Nano-micro letters., 12(1), 2020, 1-14.
11.ASHRAF, M. A., LIU, Z., PENG, W. X., JERMSITTIPARSERT, K., HOSSEINZADEH, G., HOSSEINZADEH, R., Combination of sonochemical and freeze-drying methods for synthesis of graphene/Ag-doped TiO_2 nanocomposite: A strategy to boost the photocatalytic performance via well distribution of nanoparticles between graphene sheets. Ceram. Int., 46(6), 2020, 7446-7452.
12.ZHANG, W., HU, Y., LIU, J., WANG, H., WEI, J., SUN, P., WU, L., ZHENG, H., Progress of ethylene action mechanism and its application on plant type formation in crops. Saudi J. Biol. Sci., 27(6), 2020, 1667-1673.
13.WANG, M., GUO, Y., WANG, B., LUO, H., ZHANG, X., WANG, Q., ZHANG, Y., WU, H., LIU, H., DOU, S., An engineered self-supported electrocatalytic cathode and dendrite-free composite anode based on 3D double-carbon hosts for advanced Li–SeS2 batteries. J. Mater. Chem., 8(6), 2020, 2969-2983.
14.JING, P., WANG, Q., WANG, B., GAO, X., ZHANG, Y., WU, H., Encapsulating yolk-shell FeS2@carbon microboxes into interconnected graphene framework for ultrafast lithium/sodium storage. Carbon., 159, 2020, 366-377.
15.LUO, X., GUO, J., CHANG, P., QIAN, H., PEI, F., WANG, W., MIAO, K., GUO, S., FENG, G., ZSM-5@MCM-41 composite porous materials with a core-shell structure: Adjustment of mesoporous orientation basing on interfacial electrostatic interactions and their application in selective aromatics transport. Sep. Purif. Technol., 239, 2020, 116516.
16.LUO, X., HU, H., PAN, Z., PEI, F., QIAN, H., MIAO, K., GUO, S., WANG, W., FENG, G., Efficient and stable catalysis of hollow Cu9S5 nanospheres in the Fenton-like degradation of organic dyes. J. Hazard. Mater., 396, 2020, 122735.
17.YU, H., HE, Z., QIAN, G., GONG, X., QU, X., Research on the anti-icing properties of silicone modified polyurea coatings (SMPC) for asphalt pavement. Constr. Build. Mater., 242, 2020, 117793.
18. YU, H., DAI, W., QIAN, G., GONG, X., ZHOU, D., LI, X., ZHOU, X., The NOx Degradation Performance of Nano-TiO_2 Coating for Asphalt Pavement. Nanomaterials, 10(5), 2020, 897.
19.PEREIRA, L. M., CORRÊA, A. C., ROSA, M. D. F., ITO, E. N., Rheological, Morphological and Mechanical Characterization of Recycled Poly (Ethylene Terephthalate) Blends and Composite. Mater. Res., 20(3), 2017, 791-800.
20.RANE, A. V., ABITHA, V. K., Study of Mechanical, Thermal and Micro Structural Properties of EPDM/Polypropylene/Nano clay Composites with Variable Compatibilizer Dosage. J. Mater. Environ. Sci., 6(1), 2015, 60-69.
21.GHOSH, A. K., DEBNATH, S. C., NASKAR, N., BASU, D. K., NR-EPDM Covulcanization: A Novel Approach. J. Appl. Polym. Sci., 81(4), 2001, 800-808.
22.AL-MALAIKA, S., KONG, W., Reactive processing of polymers: Functionalization of ethylene propylene diene terpolymer (EPDM) in the presence and absence of a co-agent and effect of functionalized EPDM on compatibilisation of poly (ethylene terephthalate)/EPDM blends. Polym. Degrad. Stab., 90(2), 2005, 197-210.
23.JAZANI, O. M., AZAR, A. A., Blends of Poly (ethylene terephthalate) Bottle Waste with Modified Styrene Butadiene Rubber through Reactive Mixing. J. Applied. Polym. Sci., 102(2), 2006, 1615-1623.
24.AL-GAHTANI, S. A., Mechanical Properties of Acrylonitrile butadiene/ Ethylene Propylene Diene Monomer Blends: Effects of Blend Ratio and Filler Addition. J. Am. Sci., 7(8), 2011, 804-809.
25.HALIM, S. F., EL-SABBAGH, S. H., TAWFIK, M. E., The Use of Glycolysis products of Poly (ethylene terphthalate) waste as a Compatibilzer for SBR / EPDM Blend. I- In Presence of Carbon Black and Paraffinic Oil. Int. J. Innov. Res. Sci. Eng. Technol., 3, 2014, 363-372.
26.EL-NASHAR, D. E., The Compatibilization of EPDM/SBR Blends by EPDM-Graft-Styrene Copolymer. *Polym*. Plast. *Technol.* Eng., 43(5), 2005, 1425-1441.

27.VISHVANATHPERUMAL, S., GOPALAKANNAN, S., Swelling Properties, Compression Set Behavior and Abrasion Resistance of Ethylene-propylene-diene Rubber/Styrene Butadiene Rubber Blend Nanocomposites. Polymer, 41(3), 2017, 433-442.
28.SHARMA, P. K., UPADHYAYA, P., CHAND, N., Roleof MMT nanoclay addition on TPU / EPDM rubber blends: morphology and mechanical properties. J. Sci. Res. Phys. Math. Sci., 2, 2015, 15-26.
29.NASERI, A. S. Z., JALALI-ARANI, A., A comparison between the effects of gamma radiation and sulfur cure system on the microstructure and crosslink network of (styrene bu- tadiene rubber/ethylene propylene diene monomer) blends in pre- sence of nanoclay. Rad. Phys. Chem., 115, 2015, 68–74.
30.ZHANG, K., JIANG, L., WU, G., Co-continuity and thermal expansion of injection-molded EPDM/PP blends with heterogeneous dispersion of nanoparticles. Compos. Sci. Technol., 125, 2016, 123-131.
31.DAS, A., MAHALING, R. N., STÖCKELHUBER, K. W., HEINRICH, G., Reinforcement and migration of nanoclay in polychloroprene/ethylene–propylene– diene-monomer rubber blends. Compos. Sci. Technol., 71, 2011, 276–281.
32.ENTEZAM, M., KHONAKDAR, H. A., YOUSEFI, A. A., JAFARI, S. H., WAGENKNECHT, U., HEINRICH, G., On nanoclay localization in polypropylene/poly (ethylene terephthalate) blends: Correlation with thermal and mechanical properties. Mater. Des., 45, 2013, 110–117.
33.JEDDI, J., YOUSEFZADE, O., BABAEI, A., GHANBAR, S., ROSTAMI, A., Morphology, micro-structure and rheological properties of SAN (styrene-acrylonitrile)/EPDM (ethylene-propylene-diene monomer) nanocomposites: Investigating the role of organoclay type and order of mixing. Mater. Chem. Phys., 187, 2017, 191-202.
34.BAZLI, L., KHAVANDI, A., BOUTORABI, M. A., KARRABI, M., Correlation between viscoelastic behavior and morphology of nanocomposites based on SR/EPDM blends compatibilized by maleic anhydride. Polymer, 113, 2017, 156-166.
35.YU, H., ZHU, X., QIAN, G., GONG, X., NIE, X., Evaluation of phosphorus slag (PS) content and particle size on the performance modification effect of asphalt. Constr. Build. Mater., 256, 2020, 119334.
36. LIN, J., WANG, Y., WEI, X., KONG, S., LIU, Z., LIU, J., ZHANG, F., LIN, S., JI, B., ZHOU, Z., GUO, Z., Controllable antibacterial and bacterially anti-adhesive surface fabricated by a bio-inspired beetle-like macromolecule. Int. J. Boil. Macromole., 157, 2020, 553-560.
37.LIN, J., CAI, X., LIU, Z., LIU, N., XIE, M., ZHOU, B., WANG, H., GUO, Z., Anti-liquid-Interfering and Bacterially Antiadhesive Strategy for Highly Stretchable and Ultrasensitive Strain Sensors Based on Cassie-Baxter Wetting State. Adv. Funct. Mater., 30(23), 2020, 2000398.
38.YAN, H., XUE, X., CHEN, W., WU, X., DONG, J., LIU, Y., WANG, Z., Reversible Na+ insertion/extraction in conductive polypyrrole-decorated NaTi2(PO4)3 nanocomposite with outstanding electrochemical property. Appl. Surf. Sci., 530, 2020, 147295.
39. SU, F., JIA, Q., LI, Z., WANG, M., HE, L., PENG, D., SONG, Y., ZHANG, Z., FANG, S., Aptamer-templated silver nanoclusters embedded in zirconium metal–organic framework for targeted antitumor drug delivery. Micropor. Mesopor. Mater., 275, 2019, 152-162.
40. HE, L., LIU, J., LIU, Y., CUI, B., HU, B., WANG, M., TIAN, K., SONG, Y., WU, S., ZHANG, Z., PENG, Z., DU, M., Titanium dioxide encapsulated carbon-nitride nanosheets derived from MXene and melamine-cyanuric acid composite as a multifunctional electrocatalyst for hydrogen and oxygen evolution reaction and oxygen reduction reaction. Appl. Catal. Environ., 248, 2019, 366-379.
41. WANG, M., HU, M., LIU, J., GUO, C., PENG, D., JIA, Q., HE, L., ZHANG, Z., DU, M., Covalent organic framework-based electrochemical aptasensors for the ultrasensitive detection of antibiotics. Biosens. Bioelectron., 132, 2019, 8-16.
42.KARGER-KOCSIS, J., Recycling Options for Post-Consumer PET and PET-Containing Wastes by Melt Blending: Sections 3–5. Handbook of Thermoplastic Polyesters: Homopolymers, Copolymers, Blends, and Composites, 2005, 1304-1318.
43.ZIMMERMAN, H., KIM, N. T., Investigation on thermal and hydrolytic degradation of poly (ethylene terephthalate). Polym. Eng. Sci., 20(10), 1980, 680-683.

44.CERVANTES-UC, J. M., CAUICH-RODRÍGUEZ, J. V., VÁZQUEZ-TORRES, H., GARFIAS-MESÍAS, L. F., PAUL, D. R., Thermal Degradationof Commercially Available Organoclays Studied by TGA-FTIR. Thermochim. Acta., 457(1-2), 2010, 92-102.
45.JIA, Q., LI, Z., GUO, C., HUANG, X., KANG, M., SONG, Y., HE, L., ZHOU, N., WANG, M., ZHANG, Z., FU, G., DU, M,. PEGMA-modified bimetallic NiCo Prussian blue analogue doped with Tb(III) ions: Efficiently pH-responsive and controlled release system for anticancer drug. Chem. Eng. J., 389, 2020,124468.
46. LIAO, Q., WEI, W., ZUO, H., LI, X., YANG, Z., XIAO, S., WU, G., Interfacial bonding enhancement and properties improvement of carbon/copper composites based on nickel doping. Compos. Interface., 2020, 1-13.
47. GUO, H., QIAN, K., CAI, A., TANG, J., LIU, J., Ordered gold nanoparticle arrays on the tip of silver wrinkled structures for single molecule detection. Sens. Actuators. Chem., 300, 2019, 126846.
48. GUO, H., LI, X., ZHU, Q., ZHANG, Z., LIU, Y., LI, Z.,WEN, H., LI, Y., TANG, J., LIU, J., Imaging nano-defects of metal waveguides using the microwave cavity interference enhancement method. Nanotechnology, 31(45), 2020, 455203.
49. LIU, Q., SONG, Z., HAN, H., DONKOR, S., JIANG, L., WANG, W., CHU, H., A novel green reinforcement corrosion inhibitor extracted from waste Platanus acerifolia leaves. Constr. Build. Mater., 260, 2020, 119695.
50. LIU, C., HUANG, X., WU, Y., DENG, X., LIU, J., ZHENG, Z., HUI, D., Review on the research progress of cement-based and geopolymer materials modified by graphene and graphene oxide. Nanotechnology, 9(1), 2020, 155-169.
51. JIANG, Q., SHAO, F., GAO, W., CHEN, Z., JIANG, G., HO, Y, S., Unified No-Reference Quality Assessment of Singly and Multiply Distorted Stereoscopic Images. IEEE Trans. Image. Process., 28(4), 2019, 1866-1881.
52. SHI, M., XIAO, P., LANG, J., YAN, C., YAN, X., Porous g-C3N4 and MXene Dual-Confined FeOOH Quantum Dots for Superior Energy Storage in an Ionic Liquid. Adv. Sci., 7(2), 2020.
53. SHI, M., NARAYANASAMY, M., YANG, C., ZHAO, L., JIANG, J., ANGAIAH, S., YAN, C., 3D interpenetrating assembly of partially oxidized MXene confined Mn–Fe bimetallic oxide for superior energy storage in ionic liquid. Electrochimica Acta, 334, 2020, 135546.
54.YIN, H., YU, D., Study on microstructure of PET/nanopowder composites. J. Appl. Polym. Sci., 113(1), 2009, 306-315.
55.GOUDARZI, L., IZADI-VASAFI, H. NIKFAR, N., Investigation of the morphological and mechanical properties of polyethylene terephthalate (PET)/ethylene propylene diene rubber (EPDM) blends in the presence of multi-walled carbon nanotubes. J. Macromol. Sci. B., 57(8), 2018, 585-594.

Manuscript received: 14.06.2020